J. Biochem. 2011;149(1):27–33 doi:10.1093/jb/mvq110

JB THE JOURNAL OF BIOCHEMISTRY

Synthesis of butyl-isobutyl-phthalate and its interaction with α-glucosidase *in vitro*

Received July 12, 2010; accepted September 13, 2010; published online September 23, 2010

Ming Liu[1], Wei Zhang[2], Lin Qiu[3] and Xiukun Lin[1,*]

[1]Institute of Oceanology, Chinese Academy of Science, Qingdao 266071, China, [2]Southern Research Institute, Birmingham, Alabama 35205, USA and [3]Institute for Nutritional Sciences, Shanghai Institute for Biological Sciences, Chinese Academy of Sciences, Shanghai 200031, China

*Dr Xiukun Lin, Institute of Oceanology, Chinese Academy of Sciences, 7 Nanhai Road, Qingdao, 266071, P. R. China. Tel.: +86 532 82898916, Fax: +86 532 82898916, email: linxiukun@yahoo.com

Butyl-isobutyl-phthalate (BIP), isolated from the rhizoid of *Laminaria japonica*, is a potential α-glucosidase inhibitor for Type II diabetes treatment. In the present study, a synthetic route was established as a useful approach to obtain enough BIP. Fluorescence analysis, circular dichroism spectra and molecular docking methods were employed to elucidate the underlying molecular mechanisms of BIP inhibition on α-glucosidase. The results revealed that BIP could be synthesized in two steps and the synthesized BIP bound with α-glucosidase and induced conformational changes of the enzyme. The interaction between BIP and α-glucosidase was driven by both hydrophobic forces and hydrogen bond. The docking results indicated that the benzene ring and the isopropyl group of the BIP could fit into the hydrophobic pocket composed of Phe177, Phe157, Leu176, Leu218, Ala278 and the propyl group fitted into another nearby hydrophobic pocket formed by Trp154, Pro240, Leu174 and Ala162, respectively. This study provides useful information for the understanding of the BIP-α-glucosidase interaction and development of new α-glucosidase inhibitors.

Keywords: butyl-isobutyl-phthalate/α-glucosidase/interaction/docking simulation.

Abbreviations: BIP, butyl-isobutyl-phthalate; bis-ANS, bis-8-anilinonaphthalene-1-sulfonate; CD, circular dichroism; DBP, dibutyl phthalate; DMF, dimethylformamide; IFD, induced-fit-docking.

α-Glucosidase is an enzyme that plays a central role in carbohydrate digestion and the processing of glucoproteins and glycolipids. The enzyme is also involved in diabetes, viral infection (*1*) and cancer formation (*2*). Much attention has been given to α-glucosidase as a preferred drug target in the pharmaceutical community. The clinically used α-glucosidase inhibitors, including acarbose (*3*), voglibose and miglitol (*4*), bind the α-glucosidase reversibly, and competitively inhibit α-glucosidase in the brush border in the small intestine, and consequently delay the hydrolysis of carbohydrates. However, these glycosidic derivative inhibitors showed some adverse effects. For example, acarbose usually lead to diarrhoea and abdominal discomfort by increasing the intestinal gas production (*5*, *6*) and may induce hepatotoxicity in chronic therapy (*7*). The adverse effects of miglitol include flatulence, diarrhoea, and abdominal pain, though they are mild and transitory (*8*). It is therefore necessary to develop novel α-glucosidase inhibitors with no or less adverse effects. The needs for diverse α-glucosidase inhibitors promote the search for novel classes of inhibitors. Recently, a number of α-glucosidase inhibitors have been discovered and studied (*9*–*13*). Some of these inhibitors competitively or non-competitively bind the enzyme at different sites of α-glucosidase (*14*, *15*), inducing conformational changes (*9*, *16*). While information regarding the interaction between α-glucosidase and its inhibitors could provide more insight into the structure-activity relationship, very limited effort has been contributed to explore the interaction between these newly identified inhibitors and the enzyme, and also little is known on the binding sites for the non-competitive inhibitors in α-glucosidase.

Laminaria japonica is a raw material for the production of iodine, mannitol, alginates and adsorbent (*17*), and the rhizoid of *L. japonica* has been used as a remedy for diabetes for a long time in China. In our previous study, a compound with obvious α-glucosidase inhibitory activity, butyl-isobutyl-phthalate (BIP, Fig. 1), was isolated from the rhizoid of *L. japonica* (*18*). BIP was demonstrated as a significant inhibitory agent against α-glucosidase in a concentration-dependent, non-competitive manner *in vitro*, with an IC_{50} value of 38 μM. *In vivo*, the purified BIP displayed a significant hypoglycaemic effect in streptozocin-induced diabetic mice (*18*). Our preliminary work indicated that BIP could be developed as an anti-diabetes agent for Type II diabetes therapy. However, the molecular mechanisms underlying the α-glucosidase inhibition by BIP have yet to be illustrated. Further study is needed to address the interaction between BIP and α-glucosidase. Additionally, since the content of BIP in rhizoid of *L. japonica* is very low, it is useful to develop an approach to synthesize the BIP artificially.

In this study, BIP was synthesized and the interaction of BIP with α-glucosidase was investigated by fluorescence and circular dichroism (CD) spectroscopy. Additionally, molecular modelling approaches were employed to identify the potential interactions between BIP and α-glucosidase.

Materials and Methods

Materials

The baker's yeast α-glucosidase (EC 3.2.1.20), *p*-nitrophenyl glycosides, and bis-8-anilinonaphthalene-1-sulfonate (bis-ANS) were purchased from Sigma-Aldrich Chemical, (St Louis, MO, USA). Phthalic anhydride and 1-bromo-2-methylpropane were the products of J&K Chemical Ltd (Beijing, China). All other reagents were reagent grade available.

Synthesis and characterization of BIP

The synthetic route for synthesizing BIP is shown in Scheme 1. Phthalic anhydride (3.72 g, 25 mmol) was added in 50 ml of *n*-butanol, and 1 ml of 95% H_2SO_4 was added. This mixture was refluxing over 4 h. Then, the reaction was cooled down to room temperature and 50 ml of cool water was added. The mixture was extracted by 100 ml EtOAc for three times and then the organic phase was dried over Na_2SO_4. After filtration and concentration, a compound (1) (3.5 g, 62.8%) was obtained as colourless and clear oil.

The compound (1) (3.5 g) was added in 40 ml of dry DMF, and then 1-bromo-2-methylpropane (3.25 g, 23.6 mmol) and K_2CO_3 (4.33 g, 31.4 mmol) were added. The reaction mixture was stirred at 60°C overnight. After cooling to room temperature, the mixture was diluted with H_2O (60 ml), extracted with EtOAc (60 ml × 3) and the organic layer was dried over Na_2SO_4. After filtration and concentration, the crude residue was purified by flash chromatography (10 : 1 petroleum ether/EtOAc) yielding the target compound (2) (2.00 g, 7.19 mmol, 45.8%) as colorless oil. The structure of compound (2) was characterized using TOF-MS-ES spectra, ^1H and ^{13}C NMR. The inhibitory activity of compound (2) against α-glucosidase was studied by the methods as described earlier (*18*).

Intrinsic fluorescence measurements and quenching studies

The α-glucosidase (5 μM) was pretreated with certain concentrations of BIP (0 – 400 μM) for 30 min at 37 or 25°C. The intrinsic fluorescence spectra were measured with a Cary Eclipse fluorescence spectrophotometer (Varian Inc., USA) using a standard 10 mm path-length cuvette. The excitation wavelength was 295 nm and emission spectra were acquired by scanning from 300 to 400 nm.

The dynamic quenching constant (K_{sv}) and the rate constant in the process of double molecular quenching (K_q) were calculated by plotting $\lg F_0/F$ versus $\lg[Q]$ according to the Stern–Volmer eqn. (1) as follows (*19*, *20*).

$$F_0/F = 1 + K_{sv}[Q] = 1 + Kq\tau_0[Q] \quad (1)$$

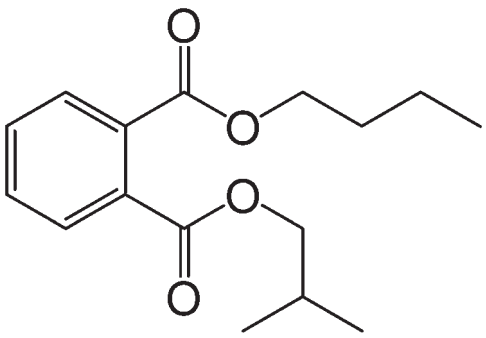

Fig. 1 Structure of BIP.

where F_0 and F are fluorescence intensity of α-glucosidase treated without or with BIP, [Q] is the concentration of BIP, τ_0 ($\sim 10^{-8}$ s) is the average life of fluorescent molecule without quencher (*20*).

The fluorescence intensity was determined with the quencher concentration through eqn. (2) (*21*, *22*). Binding constant (K_A) and binding sites (n) at 37 or 25°C were obtained through the plots of $\lg[(F_0 - F)/F]$ versus $\lg[Q]$ (*23*).

$$\lg(F_0 - F)/F = \lg K_A + n \lg[Q] \quad (2)$$

In eqn. (2), F_0 and F are fluorescence intensity of α-glucosidase treated without or with BIP; $[Q]$ is the concentration of BIP.

Thermodynamic parameters ΔH and ΔS (changes in enthalpy and entropy) were calculated by the following thermodynamic equations (*24*), where K, K_1 and K_2 value was obtained by above calculation.

$$\Delta G = \Delta H - T\Delta S, \quad (3)$$

$$\Delta G = -RT\ln K, \quad (4)$$

$$\ln(K_2/K_1) = (1/T_1 - 1/T_2)\Delta H/R. \quad (5)$$

Hydrophobic analysis of α-glucosidase using bis-ANS

α-Glucosidase (2 μM) was incubated at 37°C for 30 min in the absence or presence of certain concentrations of BIP (20 – 80 μM). Bis-ANS (15 μM) was then added, and fluorescence was measured after incubation at 37°C for 15 min ($\lambda_{ex} = 400$ nm, $\lambda_{em} =$ 450–600 nm) using FlexStation II microplate spectrofluorometer (Molecular Devices, USA).

CD spectroscopy

Far UV CD spectra (180–250 nm) of α-glucosidase treated with or without BIP were measured with a JASCO 715 spectropolarimeter (JASCO, Tokyo, Japan). All measurements were performed in 20 mM potassium phosphate buffer (pH 6.8) at 37°C. The spectra were collected and corrected by subtraction of a blank containing 20 mM potassium phosphate buffer (pH 6.8), reduction of noise and smoothing. The program JWSSE (JASCO) was used for estimation of the secondary structure of α-glucosidase based on the method of Yang *et al.* (*25*).

Molecular modelling and docking

The three-dimensional (3D) homology model of *Saccharomyces cerevisiae* α-glucosidase was constructed using the crystal structure of *Bacillus cereus* oligo-1,6-glucosidase (PDB ID: 1UOK) as structure template. There is 38% sequence identity between *S. cerevisiae* α-glucosidase and *B. cereus* oligo-1,6-glucosidase, and also 59% of their residues are positively matches according to the BLOSUM62 similarity matrix. Therefore, *B. cereus* oligo-1,6-glucosidase is a suitable structure template for the model construction of α-glucosidase. Sequence alignment of structure model building was performed using the protein structure prediction suite Prime (Schrödinger, New York, NY, USA). The homology model was further optimized using the protein preparation wizard of maestro 8.0 with OPLS2001 force field (*26*). Docking studies were performed with Induced-Fit-Docking (IFD) workflow (*27*) which is capable of sampling dramatic side-chain conformational changes as well as minor changes in the backbone structure. Ligands (BIP) were first manually docked to the active site near the centre of the catalytic triad comprised of Asp214, Glu276 and Asp349. The IFD protocol was then applied on this manually docked complex structure using the default parameter settings. Docking was carried out using rotamer libraries to sample energetically reasonable side chains and to eliminate conformations with steric crashes. The docked protein–ligand complexes were ranked according to the IFD score made up of the

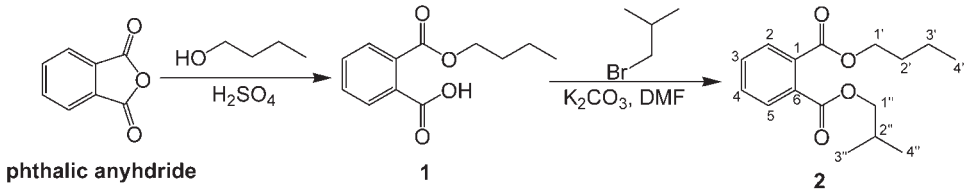

Scheme 1 Synthetic route for BIP.

protein–ligand interaction energy (GlideScore) (Schrödinger, L. Glide. New York, NY) and the protein molecular mechanics energy (Prime energy) in an implicit solvation model (*27*).

Results

Synthesis and identification of BIP

In order to obtain enough amount of BIP, we initially perform a synthetic study of BIP. The synthetic route used to synthesize BIP was shown in Scheme 1. As the starting material, phthalic anhydride was treated with butan-1-ol on the condition of H_2SO_4, to furnish 2-(butoxycarbonyl) benzoic acid (1) with yield 62.8%. Then, after alkylation with 1-bromo-2-methylpropane under basic condition of K_2CO_3 in DMF, the target compound (2) was obtained, with a yield of 45.8%. The structure of compound (2) was conformed by the following detailed spectroscopic analysis: TOF-MS-ES spectra at m/z 301.1 $[M+Na]^+$. ^1H NMR (300 MHz, $CDCl_3$) δ: 7.64 (2H, m, H-2, 5), 7.42 (2H, m, H-3, 4), 4.22 (2H, t, $J=6.6$ Hz, H-1′), 4.0 (2H, d, $J=6.9$ Hz, H-1″), 1.97 (1H, m, H-2″), 1.35 (2H, m, H-3′), 1.62 (2H, m, H-2′), 0.90 (6H, d, $J=6.6$ Hz, H-3″, H-4″), 0.85 (3H, t, $J=7.2$ Hz, H-4′); ^{13}C NMR (75 MHz, $CDCl_3$) δ: 132.1 (C-1, 6), 130.5 (C-2, 5), 128.5 (C-3, 4), 71.3 (C-1″), 65.1 (C-1′), 30.3 (C-2′), 27.4 (C-2″), 18.8 (C-3″), 18.8 (C-4″), 18.8 (C-3′), 13.3 (C-4′). According to these spectral data, the synthesized compound was identified as BIP.

The inhibitory property of synthesized BIP as an α-glucosidase inhibitor was evaluated. The synthesized BIP exhibited significant, concentration-dependent inhibitory activity against α-glucosidase with an IC_{50} value = 35 μM (data not shown), which was consistent with the BIP isolated from *L. japonica* rhizoid (*18*). These results suggested that the synthesized BIP is identical with BIP isolated from *L. japonica* rhizoid.

Intrinsic fluorescence quenching induced by BIP

Intrinsic fluorescence quenching is a valuable and versatile method for studying protein-ligand interactions (*28*). The quenching of protein fluorescence mainly depends on the exposure of tryptophan (Trp) residue to the polar and aqueous solvent (*29*). As shown in Fig. 2a, the fluorescence emission spectrum of α-glucosidase incubated with or without BIP was determined at $\lambda_{ex}=295$ nm, 37°C. When excitated at 295 nm, BIP had no obvious fluorescence emission from 300 to 400 nm. Therefore the fluorescence interference contributed from BIP was negligible. α-Glucosidase had a fluorescence peak at near 345 nm, which belongs to Trp residues of α-glucosidase (Fig. 2a). However, while α-glucosidase was incubated with BIP, the fluorescence intensity of α-glucosidase was quenched gradually with the increasing concentrations of BIP. These results suggest that there is an interaction between BIP and α-glucosidase, and that the interaction results in a microenvironment variation for Trp residues and a conformational change in α-glucosidase.

To further study the property of interaction between BIP and α-glucosidase, we next calculated the thermodynamic parameters. The values of K_{sv} and K_q were obtained by plotting F_0/F versus $[Q]$ according to Stern–Volmer eqn. (1) (Fig. 2b). As shown in Table I, the values of K_q at 25 and 37°C were more than 2.0×10^{10} per mol/s and K_{sv} (25°C) > K_{sv} (37°C). According to the methods to distinguish dynamic quenching from static quenching (*23*), BIP induced quenching was evaluated as the static quenching by forming a BIP-α-glucosidase complex. Furthermore, binding constant (K_A) and binding sites (n) were obtained through plotting $\lg[(F_0-F)/F]$ versus $\lg[Q]$ according to eqn. (2) (Fig. 2c). As shown in Table I, the value of K_A at 25 and 37°C was 4528.9 and 1524.4 (l/mol), respectively, and only one binding site was found on α-glucosidase molecule, indicating that one BIP molecule binds to the enzyme.

To further assess the interaction between BIP and α-glucosidase, the changes in enthalpy (ΔH) and entropy (ΔS) were calculated according to eqns. (3–5). As shown in Table I, the values of ΔG were negative, while ΔH and ΔS were positive. This results indicated that the interaction between α-glucosidase and BIP is a spontaneous process with increasing entropy and driven mainly by hydrophobic force.

BIP reduced hydrophobicity of α-glucosidase

Bis-ANS is a useful probe in measuring surface hydrophobicity of proteins due to its own hydrophobicity and environmental sensitivity (*30*). To study the changes in hydrophobic surface of α-glucosidase, bis-ANS was employed in the present study. The relative fluorescence intensities ($\lambda_{ex}=395$ nm, $\lambda_{em}=$ 450–600 nm) were obtained and shown in Fig. 3. BIP alone or BIP incubated with bis-ANS gave negligible fluorescence intensities, suggesting there was no interaction between BIP and bis-ANS. In contrast, with increasing concentrations of BIP, the enzyme--bis-ANS fluorescence was reduced in a concentration dependent manner (Fig. 3). These results suggest that BIP could reduce the hydrophobic surface of α-glucosidase.

Influence of BIP on the secondary structures of α-glucosidase

In order to study the influence of BIP on the secondary structure of α-glucosidase, CD spectra of the α-glucosidase (190–250 nm) were measured. As shown in Fig. 4, a maximum at 195 nm and minima at 210, 223 nm were observed, which are typical spectral features of a protein rich in α-helix structure. Analysis of the CD spectra using JWSSE predicted that the α-helix content is 35.3% and the β-sheet content is 28.3%, respectively. When the enzyme was treated with BIP, the CD spectra were shifted and showed a decline in the percentage of α-helix and an increase in the percentage of β-sheet with the increasing of BIP concentration (Table II). These results suggest that BIP could induce changes in the secondary structure of α-glucosidase with a decline in the α-helix, which was supported by the declined hydrophobicity detected by bis-ANS probe.

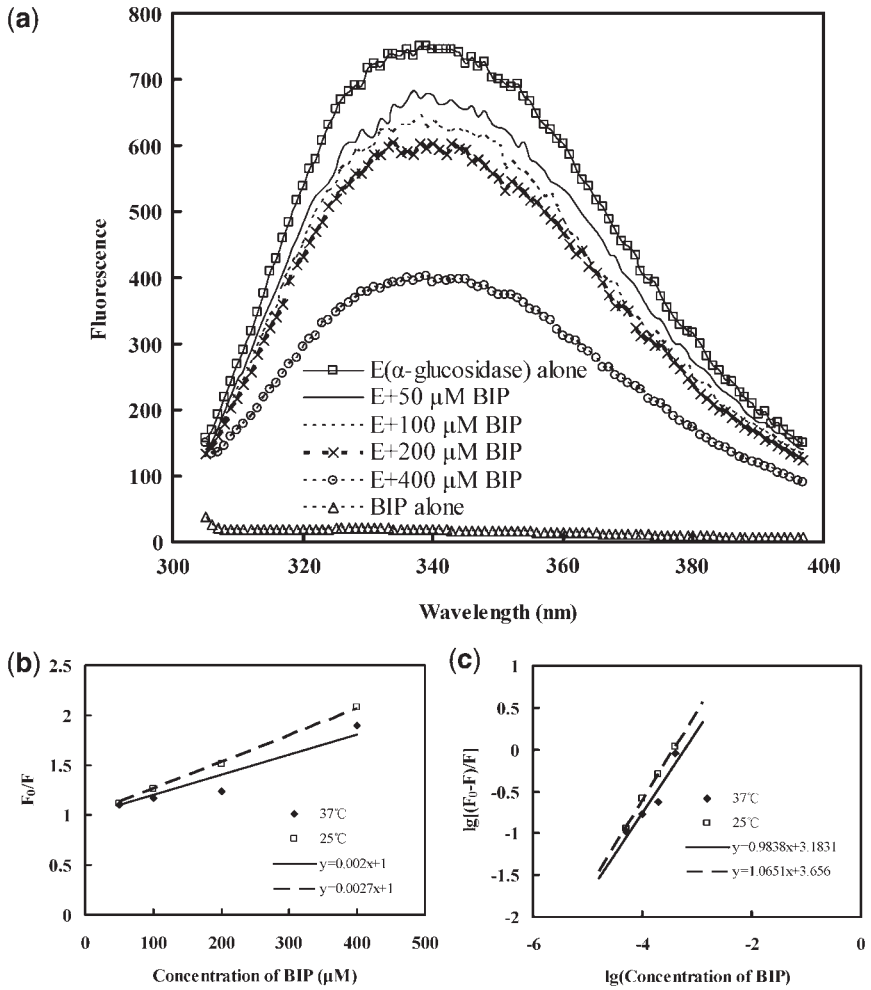

Fig. 2 Intrinsic fluorescence quenching induced by BIP. (a) Intrinsic fluorescence spectra changes of α-glucosidase by BIP. The enzyme (5 μM) was incubated with specified concentrations of BIP (0–400 μM) for 30 min at 37°C. The excitation wavelength was 295 nm and emission spectra were acquired by scanning from 300 to 400 nm. (b) Stern–Volmer plots of BIP to α-glucosidase based on fluorescence quenching at 37 and 25°C. (c) Plots of lg[$(F_0-F)/F$] versus lg[Concentration of BIP].

Table I. Constants/parameters obtained from the intrinsic fluorescence data.

Constants/parameters	25°C	37°C
K_{sv}/(l/mol)	2671.5	2025.6
$K_q/10^{11}$(l/mol/s)	2.671	2.025
K_A/(l/mol)	4528.9	1524.4
Binding sites (n)	1.0651	0.9838
ΔH/(J/mol)	303.921	303.921
ΔG/(J/mol)	−20,858.1	−18,160.1
ΔS/(J/mol/K)	69.9	59.6

The values of dynamic quenching constant (K_{sv}) and the rate constant in the process of double molecular quenching (K_q) were obtained by plotting F_0/F versus [Q] according to Stern–Volmer eqn. (1); binding constant (K_A) and binding sites (n) were obtained through plotting lg[$(F_0-F)/F$] versus lg[Q] according to eqn. (2); the changes in enthalpy (ΔH) and entropy (ΔS) were calculated according to eqns. (3–5).

Protein 3D structure generation and molecular docking

Since the 3D structure of α-glucosidase is still unavailable, a homology model was therefore developed based on the crystal structure of *B. cereus* oligo-1, 6-glucosidase (Fig. 5a). To explore the potential protein ligand interactions, docking studies were performed based on the homology model. Induced fit docking were employed to fit the ligand into the non-cognate homology structure. Interestingly, the centre of the ligand moved ~3 Å away from its starting position, which is near the catalytic triad comprised of Asp214, Glu276 and Asp349, toward the protein–solvent interface (Fig. 5b and c). Fig. 5b and c illustrated the interactions between protein and the docked top scored ligand. The benzene ring of the ligand fitted well into the hydrophobic pocket composed of Phe177, Phe157, Leu176, Leu218 and Ala278, while one of its alkyl arms (isopropyl group) bended toward the same pocket, and the other arm (propyl group) extended to fit into another nearby hydrophobic pocket formed by Trp154, Pro240, Leu174 and Ala162. Two hydrogen bonds (Fig. 5b, dotted yellow lines) formed between His239 and the carboxyl groups of ligand further strengthened the protein–ligand interactions.

As a comparison, the same docking protocol was applied on dibutyl phthalate (DBP), a BIP analogue and also a known non-competitive inhibitor of α-glucosidase (*31*). Similar binding mode was observed

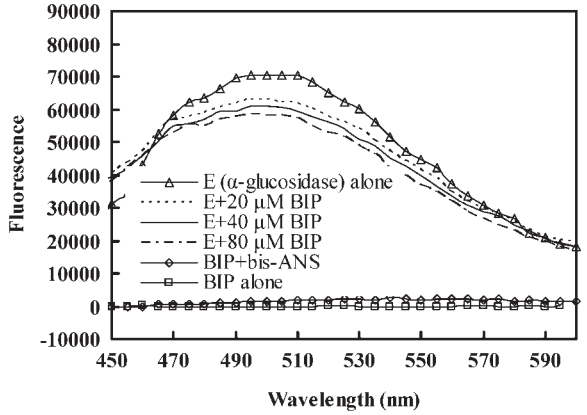

Fig. 3 Changes of α-glucosidase-bis–ANS complex fluorescence by BIP. α-Glucosidase (2 μM) was incubated for 30 min at 37°C in the absence or presence of specified concentrations of BIP (20, 40, 80 μM). Bis-ANS (15 μM) was then added, and fluorescence was measured after 15 min of incubation at 37°C (excitation at 400 nm, emission at 450–600 nm) using a Cary eclipse fluorescence spectrophotometer.

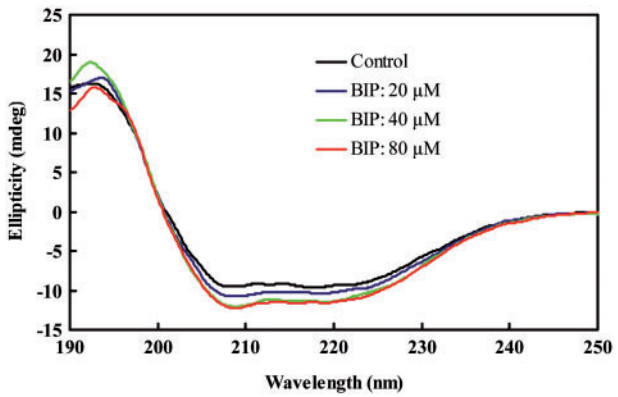

Fig. 4 CD spectra of α-glucosidase in the absence or presence of BIP. α-Glucosidase (2 μM, dissolved in 20 mM potassium phosphate buffer, pH 6.8) alone or incubated with BIP (20, 40, 80 μM) at 37°C for 30 min. Spectra were acquired from 190 to 250 nm.

from the docking results of DBP (Fig. 5d and e). Based on their docking results, the binding free energies of BIP and DBP were estimated. The calculated binding free energies were −8.08 and −8.58 kcal/mol for BIP and DBP, respectively, which was consistent with their IC_{50} values (35 and 4 μM). These docking results suggested that BIP analogues may share a common binding pocket in α-glucosidase molecule.

Discussion

In the present report, using phthalic anhydride as the start material, BIP was synthesized in two steps. From the start material to the target compounds, the total yield was 28.8%, which was more productive than the isolation method from the *L. japonica* rhizoid. The synthesized BIP exhibited the same inhibitory activity against α-glucosidase. Therefore, a valid synthesis route has been established to provide enough amount of BIP in the study of the inhibitory mechanisms, and also the synthetic approach is useful for further study of developing BIP as a possible hypoglycemic agent.

Table II. The secondary-structure content of α-glucosidase influenced by BIP.

BIP (μM)	α-Helix (%)	β-Sheet (%)	β-Turn (%)	Random (%)
0	35.3	28.3	7.4	29
20	32.6	31.6	7.1	28.7
40	31.5	32.4	7	29.1
80	27.9	33.2	10.5	28.4

The secondary structure of α-glucosidase is predicted by programme JWSSE (JASCO).

The molecular ratio is one to one in the interaction between BIP and α-glucosidase, and BIP could induce conformational changes of the enzyme; the changes in the intrinsic fluorescence as well as the hydrophobic surface of the enzyme could be found after treatment by BIP, and also the content of the secondary structure was changed with the increasing of BIP concentration. The changes in intrinsic fluorescence are similar with other studies, in which many enzymatic inhibitors could induce fluorescence quenching of their target enzymes (*23*, *32*). The decrease in the hydrophobicity supports the notion that poor hydrophobic surroundings lead to the failure of the formation of active centre. The decline in the percentage of α-helix induced by BIP is similar to other inhibitors with non-competitive inhibition manner (*9*, *33*). For example, curcuminoids isolated from *C. longa* and its analogues, as non-competitive inhibitors, also induce the decline in the percentage of α-helix of α-glucosidase (*9*). However, BIP induced decline in α-helix content is different from that of penicillamine; penicillamine is an α-glucosidase inhibitor with a mixed type of inhibition mode, and it induces an increase in the α-helix content (*34*). Penicillamine competitively binds to the catalytic domain of ligand of α-glucosidase. In contrast, the interaction between BIP and α-glucosidase is non-competitive, and may interact with different sites on α-glucosidase. These results suggested that inhibition mode on certain enzymes may be a critical factor to determine the changes of secondary structure of an enzyme. This study provides insight into understanding of interaction between α-glucosidase and its inhibitors.

In our constructed model on α-glucosidase, two hydrogen bonds were observed between His239 and the carboxyl groups of BIP with no steric hindrance between BIP and enzyme. The benzene ring and the isopropyl group of BIP molecule fitted into a hydrophobic pocket while the other arm extended to fit into another nearby hydrophobic pocket. The pocket, which fits the benzene ring and the isopropyl group of BIP molecule, is different from the binding pockets of competitive inhibitors, such as acarbose, whose binding site mainly confined to the amino acid residues in catalytic centre, including Asp214, Glu276 and Asp349 (*15*). Even after it is manually docked into the active site, BIP moved ~3 Å away from its starting position. The non-competitive inhibition

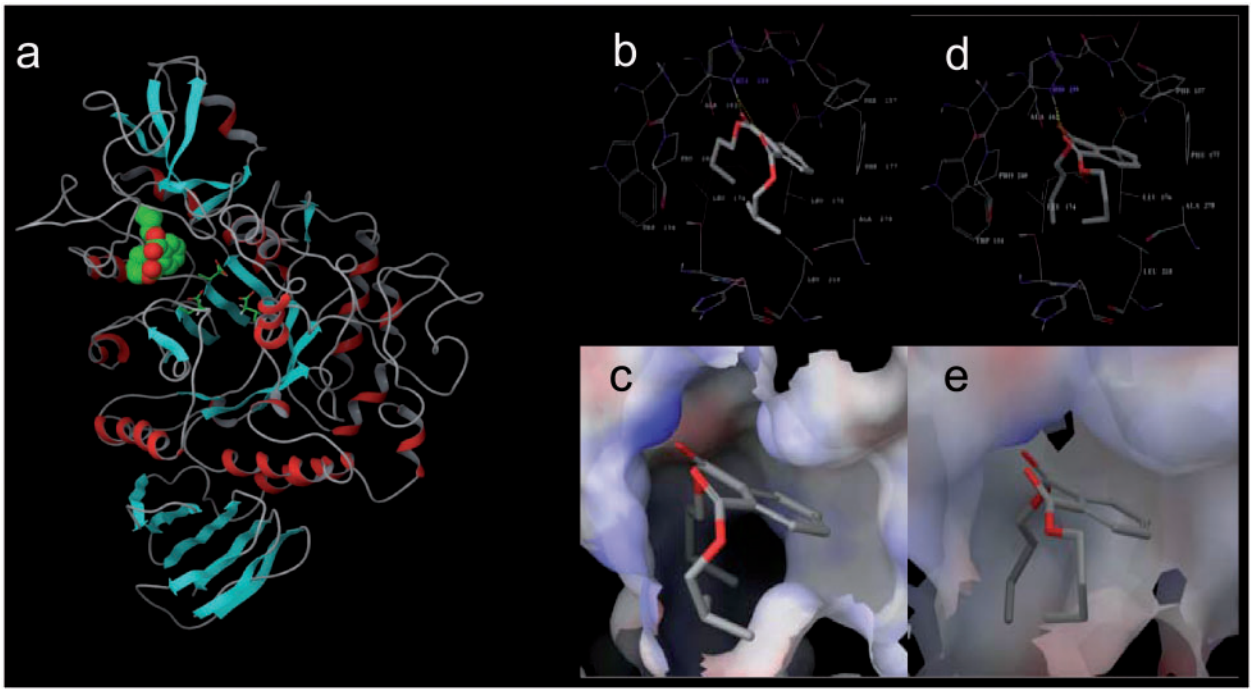

Fig. 5 Structural models of the complexes of α-glucosidase with BIP and DBP. (a) Ribbon diagram of the homology model of α-glucosidase colored by secondary structures. The docked BIP at a near surface hydrophobic pocket was included and highlighted in CPK representation; the catalytic triad residues (Asp214, Glu276 and Asp349) were displayed in sticks. (b) The interactions between the docked BIP and nearby residues. BIP were shown in solid sticks. Hydrogen bonds were marked as dotted yellow lines. (c) A close-up view of the docked BIP in protein binding pocket. The molecular surface was shown and coloured by electrostatic potentials (blue: positive; red: negative). (d) The interactions between the docked DBP and nearby residues. (e) A close-up view of the docked DBP in protein binding pocket. All graphic representations were generated using maestro 9.0 (Schrödinger, LLC, New York, NY, USA).

mode supports the results that BIP could not bind the catalytic centre of the enzyme. However, this pocket shares two residues (Phe177 and Phe157) with a hydrophobic patch comprising of Phe177, Phe157 and Tyr71, which surrounds and holds the terminal ring of acarbose (*15*). These findings suggest that Phe177 and Phe157 may have important role in the interaction between α-glucosidase and its inhibitors, and also indicates that there is at least more than one binding site other than the active centre. The predicted BIP binding site in this study provides a novel approach for designing and development of novel α-glucosidase inhibitors. Study is in progress in our lab to address if the predicted BIP binding site is a true binding site, and if it is useful as a novel targets for designing new α-glucosidase inhibitors as hypoglycemic agents.

The present clinically used α-glucosidase inhibitors, such as acarbose and miglitol, are largely confined to glycosidic derivatives which belong to competitive inhibitors. BIP is a compound structurally different from the glycosidic derivatives and inhibits α-glucosidase in a non-competitive mode. Theoretically, the inhibition effect of non-competitive inhibitors on α-glucosidase is not affected by high concentration of carbohydrates. Thus it is possible that BIP and its analogues could be developed as another class of hypoglycemic agents with little adverse effects.

In summary, BIP has been synthesized and its interaction with α-glucosidase was studied using spectroscopy and molecular modelling methods. The results revealed that BIP could bind the enzyme molecule with a ratio of one to one through hydrophobic interactions and hydrogen bonds at a novel binding site, and BIP binding could induce significant conformational changes in α-glucosidase. This study identified a novel binding site in α-glucosidase and provided new insights into the understanding of interaction between α-glucosidase and its inhibitors.

Acknowledgements

The authors would like to thank Dr Yapeng Zhang for his helpful advice regarding the synthesis of BIP.

Funding

The innovative projects of Chinese Academy of Sciences (No. KSCX2-YW-104 and KZCX2-YW-209).

Conflict of interest

None declared.

References

1. Robina, I., Moreno-Vargas, A.J., Carmona, A.T., and Vogel, P. (2004) Glycosidase inhibitors as potential hiv entry inhibitors? *Curr. Drug Metab.* **5**, 329–361
2. Humphries, M.J., Matsumoto, K., White, S.L., and Olden, K. (1986) Inhibition of experimental metastasis by castanospermine in mice: blockage of two distinct stages of tumor colonization by oligosaccharide processing inhibitors. *Cancer Res.* **46**, 5215–5222

3. Lefebvre, P.J. and Scheen, A.J. (1994) The use of acarbose in the prevention and treatment of hypoglycaemia. *Eur. J. Clin. Invest.* **24 (Suppl. 3)**, 40–44
4. Scott, L.J. and Spencer, C.M. (2000) Miglitol: a review of its therapeutic potential in type 2 diabetes mellitus. *Drugs* **59**, 521–549
5. Nathan, D.M., Buse, J.B., Davidson, M.B., Heine, R.J., Holman, R.R., Sherwin, R., and Zinman, B. (2006) Management of hyperglycaemia in type 2 diabetes: a consensus algorithm for the initiation and adjustment of therapy. A consensus statement from the american diabetes association and the european association for the study of diabetes. *Diabetologia* **49**, 1711–1721
6. Krentz, A.J. and Bailey, C.J. (2005) Oral antidiabetic agents: current role in type 2 diabetes mellitus. *Drugs* **65**, 385–411
7. Hsiao, S.H., Liao, L.H., Cheng, P.N., and Wu, T.J. (2006) Hepatotoxicity associated with acarbose therapy. *Ann. Pharmacother.* **40**, 151–154
8. Campbell, L.K., Baker, D.E., and Campbell, R.K. (2000) Miglitol: assessment of its role in the treatment of patients with diabetes mellitus. *Ann. Pharmacother.* **34**, 1291–1301
9. Du, Z.Y., Liu, R.R., Shao, W.Y., Mao, X.P., Ma, L., Gu, L.Q., Huang, Z.S., and Chan, A.S. (2006) Alpha-glucosidase inhibition of natural curcuminoids and curcumin analogs. *Eur. J. Med. Chem.* **41**, 213–218
10. Kwon, Y.I., Apostolidis, E., and Shetty, K. (2008) In vitro studies of eggplant (solanum melongena) phenolics as inhibitors of key enzymes relevant for type 2 diabetes and hypertension. *Bioresource Technol.* **99**, 2981–2988
11. Tundis, R., Loizzo, M.R., and Menichini, F. (2010) Natural products as alpha-amylase and alpha-glucosidase inhibitors and their hypoglycaemic potential in the treatment of diabetes: an update. *Mini Rev. Med. Chem.* **10**, 315–331
12. Ranilla, L.G., Kwon, Y.-I., Apostolidis, E., and Shetty, K. (2010) Phenolic compounds, antioxidant activity and in vitro inhibitory potential against key enzymes relevant for hyperglycemia and hypertension of commonly used medicinal plants, herbs and spices in latin america. *Bioresource Technol.* **101**, 4676–4689
13. Borges De Melo, E., Da Silveira Gomes, A., and Carvalho, I. (2006) [alpha]- and [beta]-glucosidase inhibitors: chemical structure and biological activity. *Tetrahedron* **62**, 10277–10302
14. Yao, X., Mauldin, R., and Byers, L. (2003) Multiple sugar binding sites in alpha-glucosidase. *Biochim. Biophys. Acta.* **1645**, 22–29
15. Bharatham, K., Bharatham, N., Park, K.H., and Lee, K.W. (2008) Binding mode analyses and pharmacophore model development for sulfonamide chalcone derivatives, a new class of alpha-glucosidase inhibitors. *J. Mol. Graph. Model* **26**, 1202–1212
16. Yoshimizu, M., Tajima, Y., Matsuzawa, F., Aikawa, S., Iwamoto, K., Kobayashi, T., Edmunds, T., Fujishima, K., Tsuji, D., Itoh, K., Ikekita, M., Kawashima, I., Sugawara, K., Ohyanagi, N., Suzuki, T., Togawa, T., Ohno, K., and Sakuraba, H. (2008) Binding parameters and thermodynamics of the interaction of imino sugars with a recombinant human acid alpha-glucosidase (alglucosidase alfa): insight into the complex formation mechanism. *Clin. Chim. Acta.* **391**, 68–73
17. Ghimire, K.N., Inoue, K., Ohto, K., and Hayashida, T. (2008) Adsorption study of metal ions onto crosslinked seaweed laminaria japonica. *Bioresour. Technol.* **99**, 32–37
18. Bu, T., Liu, M., Zheng, L., Guo, Y., and Lin, X. (2010) α-glucosidase inhibition and the *in vivo* hypoglycemic effect of butyl-isobutyl-phthalate derived from the *Laminaria japonica* rhizoid. *Phytotherapy Res.*, http://onlinelibrary.wiley.com/doi/10.1002/ptr.3139; doi:10.1002/ptr.3139 (published online 28 Jun 2010).
19. Eftink, M.R. and Ghiron, C.A. (1981) Fluorescence quenching studies with proteins. *Anal. Biochem.* **114**, 199–227
20. Lakowicz, J.R. (1999) *Principles of fluorescence spectroscopy*. 2nd edn., pp. 237–265, Plenum Press, New York
21. Lehrer, S.S. and Fasman, G.D. (1966) The fluorescence of lysozyme and lysozyme substrate complexes. *Biochem. Biophys. Res. Commun.* **23**, 133–138
22. Chipman, D.M., Grisaro, V., and Sharon, N. (1967) The binding of oligosaccharides containing n-acetylglucosamine and n-acetylmuramic acid to lysozyme. The specificity of binding subsites. *J. Biol. Chem.* **242**, 4388–4394
23. Li, Y., Gao, F., Shan, F., Bian, J., and Zhao, C. (2009) Study on the interaction between 3 flavonoid compounds and alpha-amylase by fluorescence spectroscopy and enzymatic kinetics. *J. Food. Sci.* **74**, C199–C203
24. Ross, P.D. and Subramanian, S. (1981) Thermodynamics of protein association reactions: forces contributing to stability. *Biochemistry* **20**, 3096–3102
25. Yang, J.T., Wu, C.S., and Martinez, H.M. (1986) Calculation of protein conformation from circular dichroism. *Methods Enzymol.* **130**, 208–269
26. Price, M.L.P., Ostrovsky, D., and Jorgensen, W.L. (2001) Gas-phase and liquid-state properties of esters, nitriles, and nitro compounds with the opls-aa force field. *J. Comput. Chem.* **22**, 1340–1352
27. Sherman, W., Day, T., Jacobson, M.P., Friesner, R.A., and Farid, R. (2006) Novel procedure for modeling ligand/receptor induced fit effects. *J. Med. Chem.* **49**, 534–553
28. Lee, Y.C. (1997) Fluorescence spectrometry in studies of carbohydrate-protein interactions. *J. Biochem.* **121**, 818–825
29. Burstein, E.A., Vedenkina, N.S., and Ivkova, M.N. (1973) Fluorescence and the location of tryptophan residues in protein molecules. *Photochem. Photobiol.* **18**, 263–279
30. Hawe, A., Sutter, M., and Jiskoot, W. (2008) Extrinsic fluorescent dyes as tools for protein characterization. *Pharm. Res.* **25**, 1487–1499
31. Lee, D.S. (2000) Dibutyl phthalate, an alpha-glucosidase inhibitor from Streptomyces melanosporofaciens. *J. Biosci. Bioeng.* **89**, 271–273
32. Qi, X. and Grabowski, G.A. (1998) Acid beta-glucosidase: intrinsic fluorescence and conformational changes induced by phospholipids and saposin c. *Biochemistry* **37**, 11544–11554
33. Wang, Y., Ma, L., Li, Z., Du, Z., Liu, Z., Qin, J., Wang, X., Huang, Z., Gu, L., and Chen, A.S. (2004) Synergetic inhibition of metal ions and genistein on alpha-glucosidase. *FEBS Lett.* **576**, 46–50
34. Kim, J.H., Kim, H.J., Park, H.W., Youn, S.H., Choi, D.Y., and Shin, C.S. (2007) Development of inhibitors against lipase and alpha-glucosidase from derivatives of monascus pigment. *FEMS Microbiol. Lett.* **276**, 93–98